

Homodyne estimation of quantum states purity by exploiting covariant uncertainty relation.

V.I. Man'ko,^{1,*} G. Marmo,^{2,3,4,†} A. Porzio,^{5,4,‡} S. Solimeno,^{2,6,4,§} and F. Ventriglia^{2,3,4,¶}

¹*P.N.Lebedev Physical Institute, Moscow 119991, Russia*

²*Dipartimento di Scienze Fisiche, Università "Federico II", Via Cintia, I-80126 Napoli, Italy*

³*INFN, Sezione di Napoli, Via Cintia, I-80126 Napoli, Italy*

⁴*MECENAS, Università "Federico II", Napoli, Italy*

⁵*CNR-SPIN, Complesso Universitario di Monte S. Angelo, Via Cintia, I-80126 Napoli, Italy*

⁶*CNISM, Udr Napoli, Via Cintia, I-80126, Napoli, Italy*

We experimentally verify uncertainty relations for mixed states in the tomographic representation by measuring the radiation field tomograms, *i.e.* homodyne distributions. Thermal states of single-mode radiation field are discussed in details as paradigm of mixed quantum state. By considering the connection between generalised uncertainty relations and optical tomograms is seen that the purity of the states can be retrieved by statistical analysis of the homodyne data. The purity parameter assumes a relevant role in quantum information where the effective fidelities of protocols depend critically on the purity of the information carrier states. In this contest the homodyne detector becomes an easy to handle purity-meter for the state on-line with a running quantum information protocol.

I. INTRODUCTION

Quantum pure states can be faithfully described by their wavefunction $\psi(x)$. Experimentally producing and measuring pure quantum states is impossible due to the imperfections both of the generation procedures and the measurement apparatus. In particular quantum states of the optical fields are always mixed due to impossibility of transmitting and detecting optical fields with 100% efficiencies. Density matrix $\hat{\rho}$ formalism encompasses the possibility of describing both pure and mixed state. In this context an important parameter is represented by the purity $\tilde{\pi}$ given by the trace of the squared density matrix operator with $\tilde{\pi} = 1$ for pure states while $\tilde{\pi} < 1$ for mixed ones. Moreover, $\tilde{\pi}$ assumes a relevant role in quantum information protocols [1], where the fidelity, *i.e.* the rate of success, depends critically on the purity of the states. $\tilde{\pi}$ also can give a quantitative measure of the decoherence the pure state have suffered.

Pure states satisfy the Schrödinger [2] and Robertson [3] basic inequalities that generalize Heisenberg [4] uncertainty relations including contributions from covariance of conjugate quantum observables. In Ref. [5] (see also [6]) a new bound, higher than the Schrödinger-Robertson, which accounts for the contribution of the purity of mixed states was found. In Ref. [7] the Schrödinger-Robertson uncertainty relation was expressed in terms of homodyne tomograms. The generic tomographic approach to quantum systems was reviewed in [8]. Combining the purity dependent bound and its expression in terms of homodyne tomograms give rise to a method for a simple determination of the state purity via homodyne detection developed in [9–14].

*Electronic address: manko@na.infn.it

†Electronic address: marmo@na.infn.it

‡Electronic address: porzio@na.infn.it

§Electronic address: solimeno@na.infn.it

¶Electronic address: ventriglia@na.infn.it

The problem of measuring the position and momentum was discussed also in connection with the tomographic approach recently in [16].

So far, evaluation of purity in continuous variable (CV) systems is obtained once the full state density matrix have been reconstructed by quantum tomographic methods. In this paper we prove that the purity of the analyzed state can be retrieved by a very simple and fast analysis of homodyne data thus giving the possibility of having an on-line monitor on the state.

The aim of the present paper is twofold. On the one hand we express the purity $\tilde{\pi}$ of a mixed state in terms of homodyne tomograms, *i.e.* quantities amenable to an experimental determination. On the other hand, relying on the uncertainty relations of Ref. [5] we derive a simple estimator for the purity of a thermal state which is independent from its tomographic expression.

In Ref. [17] a probability representation of quantum mechanics was suggested in which states are described by standard probability distributions, called tomograms. This representation is based on the representation of the Wigner function $W(p, q)$ of a quantum state by means of the Radon integral transform of marginal distributions (optical tomograms) [18, 19]. These data representing the output of optical homodyne detectors allows reconstructing the Wigner function using the experimental data. This tomography procedure is nowadays a routine method for measuring quantum states (see for a review [14, 15]). Using ideas discussed in [7], in the present paper we apply the optical tomography method to check generalized Schrödinger-Robertson uncertainty relations for conjugate quadratures in the case of a mixed quantum state, in particular, for measuring the effective temperature of a thermal state. The idea of our consideration is based on suggestion [17] (see, also [8]) that the homodyne tomogram is a primary object identified with the quantum state. Due to this, one can extract all information on the state properties including the purity from the measured tomogram only, avoiding the reconstruction of the Wigner function procedure.

The paper is organized as follows.

In section 2, starting from the symplectic forms we give an expression of the purity parameter and of the mean photon number of any mixed photon state in terms of measurable optical tomograms. For thermal mixed states this expression provides the temperature of the field and the mean photon number thus suggesting to check the accuracy of homodyne detection by comparing photon statistics obtained in this way, *i.e.*, from optical tomograms, and in independent photon counting experiment.

In section 3, we review mixed state uncertainty relations to get an estimation of the purity independent of its tomographic expression, by saturating the bound set by the uncertainty relation found in [5]. Hence, measuring optical tomograms of photon states, we can evaluate the purity of the state, and, in the case of thermal states, study the dependence of the quantum bound on the field temperature, thus obtaining a sort of a thermometer for evaluating the temperature. Also, we obtain an estimation for the mean photon number. Finally, in section 4, an experimental comparison, for thermal states, is performed between our estimation and an independent measure of purity of the state, which allows for evaluating the accuracy of our approximate estimation.

II. TOMOGRAM AS PURITY AND THERMAL METERS

A quantum state, either mixed or pure, is described by a density operator $\hat{\rho}$ with purity parameter $\tilde{\pi}$ given by:

$$\tilde{\pi} = \text{Tr} [\hat{\rho}^2] \leq 1 .$$

According to [17] the state is described by a symplectic tomogram $\mathcal{W}(X, \mu, \nu)$, where X, μ, ν are real parameters, obtained by the Radon transform of the Wigner function $W(p, q)$ (hereafter, $\hbar = 1$):

$$\mathcal{W}(X, \mu, \nu) = \int W(p, q) \delta(X - \mu q - \nu p) \frac{dpdq}{2\pi} = \text{Tr} \left[\hat{\rho} \delta(\hat{X} - \mu\hat{Q} - \nu\hat{P}) \right] , \quad (1)$$

with $\delta(\hat{X} - \mu\hat{Q} - \nu\hat{P})$ standing for

$$\hat{X} = \mu\hat{Q} + \nu\hat{P}$$

Accordingly the generalized quadrature operator $\hat{X}(\mu, \nu)$ depends parametrically on μ, ν and its moments are given by:

$$\langle \hat{X}^n(\mu, \nu) \rangle = \int X^n \mathcal{W}(X, \mu, \nu) dX , \quad n = 1, 2, 3, \dots$$

like means and variances, in terms of homodyne quadrature statistics. In particular,

$$\hat{X}^2(\mu, \nu) = \mu^2\hat{Q}^2 + \nu^2\hat{P}^2 + 2\mu\nu \left(\frac{\hat{Q}\hat{P} + \hat{P}\hat{Q}}{2} \right) . \quad (2)$$

so that

$$\left\langle \left(\hat{X}(\mu, \nu) - \langle \hat{X}(\mu, \nu) \rangle \right)^2 \right\rangle = \sigma_{XX}(\mu, \nu) = \mu^2\sigma_{QQ} + \nu^2\sigma_{PP} + 2\mu\nu\sigma_{PQ} \quad (3)$$

Accordingly, the mixed state is characterized by the quadrature dispersions $\sigma_{QQ}, \sigma_{PP}, \sigma_{PQ}$, which in turn can be determined by measuring $\sigma_{XX}(\mu, \nu)$ for particular values of μ, ν . In case of optical tomograms, one has $\mu = \cos\theta, \nu = \sin\theta$ so that the optical field state is characterized by the field quadratures relative to $\theta = 0, \pi/2$ and $\theta = \pi/4$:

$$\begin{aligned} \sigma_{QQ} &= \sigma_{XX}(1, 0) , \quad \sigma_{PP} = \sigma_{XX}(0, 1) , \\ \sigma_{PQ} &= \sigma_{XX}\left(\frac{\sqrt{2}}{2}, \frac{\sqrt{2}}{2}\right) - \frac{1}{2}[\sigma_{XX}(1, 0) + \sigma_{XX}(0, 1)] . \end{aligned}$$

Analogously the photon number operator $\hat{n} = \hat{a}^\dagger\hat{a} = \frac{1}{2}(\hat{Q}^2 + \hat{P}^2 - 1)$ is related to the moments

$$\langle \hat{n} \rangle = \frac{1}{2} \left[\langle \hat{X}^2(1, 0) \rangle + \langle \hat{X}^2(0, 1) \rangle - 1 \right] . \quad (4)$$

Hence the accuracy of the homodyne detection could be assessed by comparing $\langle \hat{n} \rangle$ obtained via optical tomograms with that measured by standard photon counting experiments.

The purity $\tilde{\pi}$ of $\hat{\rho}$ is a functional of $\mathcal{W}(X, \mu, \nu)$ (see, for example, [8])

$$\tilde{\pi} = \text{Tr} [\hat{\rho}^2] = \frac{1}{2\pi} \int dX dY d\mu d\nu \left[e^{i(X+Y)} \mathcal{W}(X, \mu, \nu) \mathcal{W}(Y, -\mu, -\nu) \right]$$

or equivalently

$$\tilde{\pi} = \frac{1}{2\pi} \iint dX dY \int_0^{2\pi} d\theta \int_0^\infty dk \left[k e^{ik(X+Y)} \mathcal{W}_0(X, \theta) \mathcal{W}_0(Y, \theta + \pi) \right], \quad (5)$$

having replaced $\mathcal{W}(X, \mu, \nu)$ with the homodyne marginal distribution

$$\mathcal{W}_0(X, \theta) = k \mathcal{W}(kX, k \cos \theta, k \sin \theta)$$

which is accessed in homodyne measurements.

For Gaussian photon states $\mathcal{W}(X, \mu, \nu)$ reduces to:

$$\mathcal{W}(X, \mu, \nu) = \frac{1}{\sqrt{2\pi\sigma_{XX}(\mu, \nu)}} \exp \left[-\frac{(X(\mu, \nu) - \langle X(\mu, \nu) \rangle)^2}{2\sigma_{XX}(\mu, \nu)} \right] \quad (6)$$

which inserted (6) into (5) yields the well-known expression:

$$\tilde{\pi} = \frac{1}{2\sqrt{\sigma_{QQ}\sigma_{PP} - \sigma_{QP}^2}}. \quad (7)$$

For a thermal state ($\sigma_{QQ} = \sigma_{PP} = \frac{1}{2} \coth(\frac{1}{2T})$; $\sigma_{QP} = 0$) $\tilde{\pi}$ reduces to

$$\tilde{\pi} = \tanh\left(\frac{1}{2T}\right) \quad (8)$$

with T measured in *Kelvin* $\times K_B/\hbar\omega$.

III. MIXED STATE UNCERTAINTY RELATION

The general uncertainty relation for a mixed state reads [5]

$$\sigma_{QQ}\sigma_{PP} - \sigma_{QP}^2 \geq \frac{1}{4}\Phi^2(\tilde{\pi}). \quad (9)$$

with $\tilde{\pi}$ the purity of the state $\hat{\rho}$. The real, continuous and differentiable function $\Phi(\tilde{\pi})$, such that $\Phi(\tilde{\pi}) \geq 1$ in the interval $0 < \tilde{\pi} \leq 1$, has the following piecewise analytic expression (extrema of intervals are given by $2(2k+1)/3k(k+1)$, $k = 1, 2, \dots$):

$$\begin{aligned} \Phi(\tilde{\pi}) &= 2 - \sqrt{2\tilde{\pi} - 1} & \frac{5}{9} \leq \tilde{\pi} \leq 1 \\ \Phi(\tilde{\pi}) &= 3 - \sqrt{8\left(\tilde{\pi} - \frac{1}{3}\right)} & \frac{7}{18} \leq \tilde{\pi} \leq \frac{5}{9} \\ \Phi(\tilde{\pi}) &= 4 - \sqrt{20\left(\tilde{\pi} - \frac{1}{4}\right)} & \frac{3}{10} \leq \tilde{\pi} \leq \frac{7}{18} \\ &\dots\dots\dots \end{aligned} \quad (10)$$

We generalize the inequality (9) to arbitrary local oscillator phases θ , by using the tomographic uncertainty function $F(\theta)$ introduced in [7]:

$$F(\theta) \geq \frac{1}{4} [\Phi^2(\tilde{\pi}) - 1]. \quad (11)$$

Besides, the function $\Phi(\tilde{\pi})$ can be approximated in the whole interval $(0, 1)$ within 1% by the interpolating function [5, 6]:

$$\tilde{\Phi}(\tilde{\pi}) = \frac{4 + \sqrt{16 + 9\tilde{\pi}^2}}{9\tilde{\pi}}. \quad (12)$$

In Fig. (1) we plot the relative difference between $\Phi^2(\tilde{\pi})$, the square of the bound function, and $\tilde{\Phi}^2(\tilde{\pi})$ in order to visualize how good is the approximation.

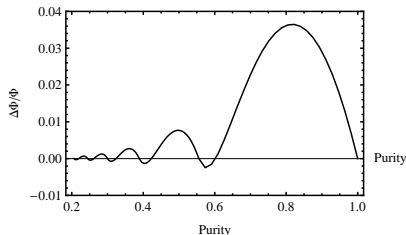


FIG. 1: Relative difference between the bound Φ^2 and its approximation $\tilde{\Phi}^2$ given in Eq. (12). $\tilde{\Phi}^2$ approximates Φ^2 within a few percents.

Then, by using $\tilde{\Phi}(\tilde{\pi})$ instead of $\Phi(\tilde{\pi})$, the uncertainty relation reads:

$$F(\theta) - \frac{1}{4} \left[\tilde{\Phi}^2(\tilde{\pi}) - 1 \right] = F(\theta) - \left[\frac{8 + 2\sqrt{16 + 9\tilde{\pi}^2} - 18\tilde{\pi}^2}{81\tilde{\pi}^2} \right] \geq 0, \quad (13)$$

in this way, a relation between the tomographic uncertainty function $F(\theta)$ and the state purity is set.

We recall that $F(\theta)$ is defined, by means of the variance of the homodyne quadrature \hat{X}

$$\sigma_{XX}(\theta) = \int X^2 \mathcal{W}_0(X, \theta) dX - \left[\int X \mathcal{W}_0(X, \theta) dX \right]^2, \quad (14)$$

as:

$$F(\theta) := \sigma_{XX}(\theta) \sigma_{XX}\left(\theta + \frac{\pi}{2}\right) + \left[\sigma_{XX}\left(\theta + \frac{\pi}{4}\right) - \frac{1}{2} \left(\sigma_{XX}(\theta) + \sigma_{XX}\left(\theta + \frac{\pi}{2}\right) \right) \right]^2 - \frac{1}{4}. \quad (15)$$

We note that for $\theta = 0$ one has

$$F(\theta)|_{\theta=0} = \sigma_{QQ} \sigma_{PP} - \sigma_{QP}^2 - \frac{1}{4}. \quad (16)$$

So that, $F(\theta)|_{\theta=0} \geq 0$ is exactly the Schrödinger-Robertson inequality. Moreover, comparing the last expression with the thermal state purity given in Eq. (7) it is easy to see that:

$$\tilde{\pi} = \frac{1}{2\sqrt{F(\theta)|_{\theta=0} + \frac{1}{4}}}.$$

The above expression of the uncertainty function $F(\theta)$ in terms of tomograms was given in [7].

The physical meaning of the function $F(\theta)$ is the following. For a local oscillator phase $\theta = 0$, it is the determinant of the quadrature dispersion matrix, shifted by $-1/4$ as shown in Eq. (16). For a nonzero local oscillator phase θ ,

the function $F(\theta)$ corresponds to the determinant of the dispersion matrix of the quadratures, which are measured in a rotated reference frame in the quadrature phase space. The non-negativity of the function $F(\theta)$ implies the fulfilling of the Schrödinger-Robertson uncertainty relation for all the unitarily equivalent position and momentum operators, since the unitary transformations do not change the canonical commutation relations. The formula (15) simply expresses the determinant of the dispersion matrix for unitarily rotated position and momentum, in terms of tomographic probability distribution $\mathcal{W}_0(X, \theta)$.

Thus, the tomogram must satisfy the inequality (11), or (13), where the parameter $\tilde{\pi}$ is expressed in tomographic terms by Eq. (5). However, we can get an estimation of the purity in terms of the tomographic uncertainty function $F(\theta)$ by saturating the inequality (13). In other words, we consider the minimum value F of the uncertainty function $F(\theta)$ and estimate that for such a value the inequality is pretty near saturated. Then, by solving with respect to $\tilde{\pi}$, we are able to express the purity as a function of F . This is a simple expression:

$$\tilde{\pi}(F) \approx \frac{2\sqrt{1+4F}}{2+9F}, \quad (17)$$

whose plot is shown in Fig. 2.

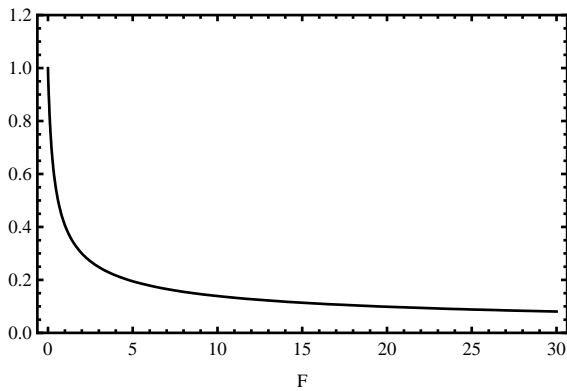


FIG. 2: Purity vs. F the minimum value of $F(\theta)$. F saturates the inequality (13).

As one can see, $F = 0$ corresponds to a pure state, $\tilde{\pi} = 1$, and the purity is a smooth decreasing function, going to zero for F at infinity.

On the other hand, for thermal states the purity parameter is directly related to the temperature, i.e. $\tilde{\pi} = \tanh(1/2T)$, so that the previous inequalities and estimations can be translated in terms of temperature. So, in particular, for a thermal state the bound $\tilde{\Phi}$ in inequality (13) can be written in terms of the temperature T .

Moreover, $F(\theta)$ provides the temperature $T(F)$ of a thermal state with the corresponding purity $\tilde{\pi}(F)$. We get

$$T = [2 \tanh^{-1} \tilde{\pi}]^{-1} \approx \left[2 \tanh^{-1} \left(\frac{2\sqrt{1+4F}}{2+9F} \right) \right]^{-1}. \quad (18)$$

We recall that for a thermal state the tomographic uncertainty function $F(\theta)$ does not depend on the local oscillator phase θ , as shown in [7], so that $F(\theta) = F, \forall \theta$.

Finally, we remark that for a thermal state the mean value of the photon number can be expressed as a function of

the temperature as

$$\langle \hat{n} \rangle = \frac{1}{2} \coth \left(\frac{1}{2T} \right) - \frac{1}{2}, \quad (19)$$

so we have a relation between our estimation of the temperature $T(F)$ and the photon statistics.

In other words, we may check the accuracy of our estimation of the purity and the temperature, resulting from inequality (13), by comparing our estimation of $\langle \hat{n} \rangle$, i.e.

$$\langle \hat{n} \rangle (F) = \frac{2 + 9F}{4\sqrt{1 + 4F}} - \frac{1}{2}, \quad (20)$$

with an independent measure of the mean number of photons. This comparison is discussed in the next section.

We conclude this section by observing that if the state is not thermal, but we succeed in finding the value F saturating the uncertainty inequality to introduce an effective temperature T_{eff} . This effective temperature is again given by the right hand side of Eq. (18) and corresponds to a purity parameter $\tilde{\pi}(F)$.

IV. EXPERIMENT

Since the uncertainty relations have been written in terms of optical tomograms experimental data obtained by optical homodyne detector are suitable for retrieving $F(\theta)$, thus checking the uncertainty relation (13) and, in case of a thermal state, evaluate $\tilde{\pi}$, the state purity (Eq. (17)), T , the effective field temperature (Eq. (18)), and $\langle \hat{n} \rangle$, the mean photon number (Eq. (20)). Then, in order to assess the reliability of the proposed method, it is possible to compare the estimations of $\tilde{\pi}$ with the same quantity obtained via quantum tomographically reconstructing the quantum state and by using Eq. (7).

$F(\theta)$ has been retrieved for thermal continuous wave (CW) modes, outputting a sub-threshold non-degenerate optical parametric oscillator (OPO) [20]. In such a device non-linear fluorescence give rise to a pair of down-converted entangled mode each in a thermal state [21]. The experimental setup, illustrated in greater details elsewhere [20, 21], can be sketched into three distinct blocks: the state source, a below threshold OPO, the detector, a quantum homodyne and related electronics, and the, PC based, acquisition board.

The quantum homodyne detector, shows an overall quantum efficiency $\eta = 0.88 \pm 0.02$ (see Refs. [12, 22, 23] for details). The system is set to obtain a 2π -wide linear scanning of the LO phase in an acquisition window. Since $F(\theta)$ is retrieved by combining variances of data distributions calculated at different θ , and in order to avoid any problem due to a non-perfect matching between the 0 (starting) and the 2π (ending) phase we decided to retrieve $F(\theta)$ in $[0, \pi]$.

Data sampling is moved away from the laser carrier frequency by mixing the homodyne current with a sinusoidal signal of frequency $\Omega = 3$ MHz. The resulting current, low-pass filtered with a bandwidth $B = 300$ kHz, is eventually sampled by a digital acquisition PC based module (GageScope 14100) able to acquire up to 1M-points per run with 14 bits resolution.

In order to use our homodyne data to calculate $F(\theta)$, we must be sure that the state is effectively a thermal one. First we prove that the state is Gaussian by performing some tests to assess the Gaussianity of data distribution [24].

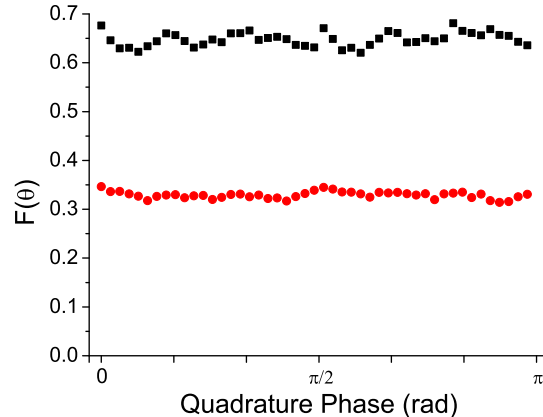


FIG. 3: $F(\theta)$ vs LO phase $\theta \in [0, \pi[$. The mean values are: 0.65 ± 0.01 (black, $\tilde{\pi} = 0.48$), and 0.329 ± 0.007 (red, $\tilde{\pi} = 0.61$) where the errors are the standard deviations of the $F(\theta)$ distributions in θ . The plotted range corresponds to 47 phase bins (see text for details).

In particular, we have used the kurtosis excess (or Fisher's index) and the Shapiro-Wilk indicator. The kurtosis is a measure of the "peakedness" of the probability distribution of a real-valued random variable while the Shapiro-Wilk one tests the null hypothesis that a distribution x_1, \dots, x_n came from a normally distributed population. Then, a pattern function tomographic analysis is used for assuring the thermal character of the state [12, 25].

$F(\theta)$ is calculated by first assigning the data at 47 phase bins each containing 2100 points (every bin corresponds to a phase interval interval of $\theta = 0.067$ rad and then, analyzing the data distributions at different θ , makes use of Eq. (15).

A typical output is reported in Fig. 3. The trace are obtained by subtracting the average F value obtained for the corresponding calibration trace, *i.e.* the shot noise trace, obtained by obscuring the homodyne input. Being homodyne data normalized so to have a shot noise variance of $1/2$; $F(\theta)$ for a shot noise trace returns the instrument 0. Furthermore, in order to avoid any influence on the statistics of the data, the electronic noise floor is kept ≈ 15 dB below the shot noise. The values of $F(\theta)$, always positive as predicted by the uncertainty relation (13), are with a good approximation independent of θ as expected for a thermal state.

We have analysed 218 homodyne acquisitions of thermal states. This large number allows a statistical approach for analysing the reliability of the proposed method. In particular the purity $\tilde{\pi}$ of the state has been evaluated: a) by reconstructing the state density matrix via homodyne tomography ($\tilde{\pi}_{tom}$); b) by using Eq. (17) ($\tilde{\pi}_F$); c) by using the exact expression for a thermal state (see Eq. (7)) ($\tilde{\pi}_{th}$). In Fig. 4 we report the values of the differences Δ_{F-tom} (a) and Δ_{th-tom} (b) between $\tilde{\pi}_F$ and $\tilde{\pi}_{tom}$ and $\tilde{\pi}_{th}$ and $\tilde{\pi}_{tom}$ normalised to their average. $\tilde{\pi}_{tom}$ has been taken as a reference [27]. By looking at these distributions it is seen that while Δ_{th-tom} is normally distributed (see inset in Fig. 4 (b)) with an average of 0.022 (standard deviation 0.018) Δ_{F-tom} presents a nearly well defined behaviour in $\tilde{\pi}$ thus signalling the insorgence of systematic error in the obtained determination. While $\tilde{\pi}_{th}$ comes from the exact expression of Eq. (7), $\tilde{\pi}_F$ come from some approximation in the formula used for $\phi(\tilde{\pi})$ (see the previous section for

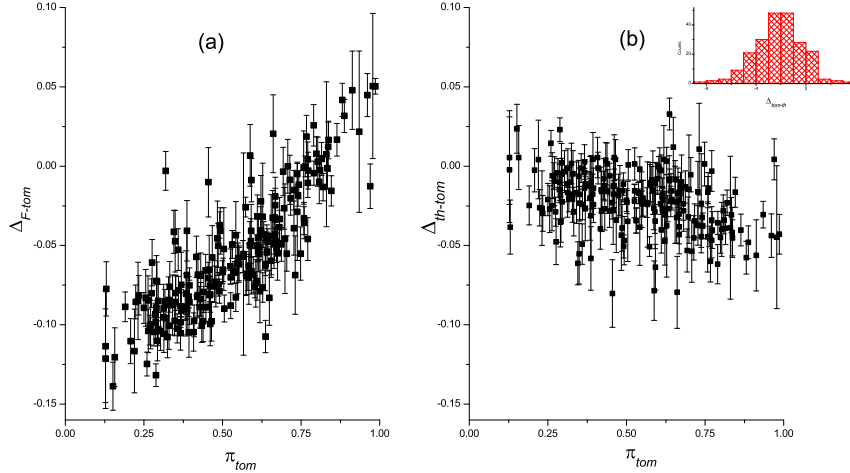


FIG. 4: Δ_{F-tom} (a) and Δ_{th-tom} (b) vs. $\tilde{\pi}_{tom}$. The histogram Δ_{th-tom} , given in the inset of (b), prove that Δ_{th-tom} is normally distributed. Δ_{F-tom} shows a well defined behaviour in $\tilde{\pi}_{tom}$ thus signalling the insorgence of systematic error due to the used approximation. The extimation become more precise for highly pure states. The maximum error is arround 15%.

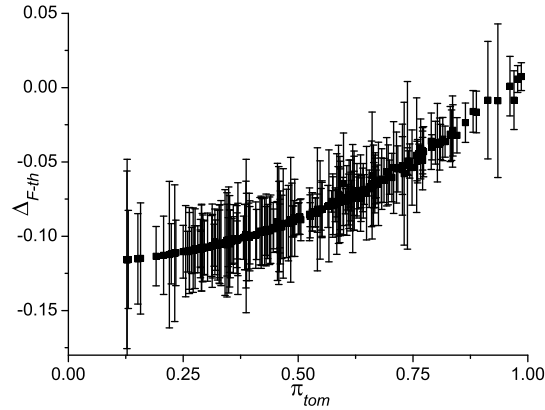


FIG. 5: Δ_{F-th} vs. $\tilde{\pi}_{tom}$. presents a very well defined behaviour in $\tilde{\pi}_{tom}$ due to systematic errors caused by the applied approximation.

details) thus, the precision depends on the purity itself. It has to noted that in any case the maximum error, for higly mixed states, remains above -0.15 .

The regular discrepancy becomes even more evident for Δ_{F-th} (see Fig. 5).

The above discussed discrepancies, even not so small, confirms that the estimation of $F(\theta)$, much more simpler than any full state reconstruction methods [14] gives many reliable information on the homodyned state. Moreover, for a thermal state it is possible to obtain more precise information by exploiting Eq. (7).

By exploiting the thermal character of the states herein analysed it is possible to get information on T (Eq. (18)) and $\langle \hat{n} \rangle$ averaging the experimental trace for $F(\theta)$ over θ . The values so obtained are given in the following table (together with their confidence interval):

mode	F	$T \frac{k_B}{\hbar \omega}$	$\langle \hat{n} \rangle$
1	0.65 ± 0.01	3.8 ± 0.1	0.53 ± 0.09
2	0.329 ± 0.007	2.8 ± 0.1	0.315 ± 0.006

(21)

The analyzed mode have $\nu \approx 3 \times 10^{14}$ Hz so that the field effective temperature is of the order $\approx 10^4$ K.

V. CONCLUSIONS

By looking at the information underlying the uncertainty relations for mixed quantum states [5, 6] and relating them to optical tomograms of the *e.m.* quantum states is possible to easily estimate the purity of mixed states. It is shown that quadrature statistics of the field contain complete information on bound in the generalized uncertainty relation of mixed state and that this bound is intimately related to the state purity. This approach gives the possibility of a fast and reliable estimation of the purity parameter for quantum states that does not require sophisticated data analysis. As far as we know, all the methods for purity estimation rely on the reconstruction of the whole state density matrix while the approach present in this paper allows to recover the purity simply calculating the tomographic function $F(\theta)$. In addition, for thermal states the suggested procedure is a new method for measuring the temperature of the electromagnetic field. The experimental results presented in the paper provided the first implication of the new method where the homodyne detector is used as the purity meter of the electromagnetic radiation in the quantum domain. The experimental estimations obtained via $F(\theta)$ are compatible with more sophisticated estimation obtained via pattern function tomography so proving that our method can be used for real-time evaluations of some basic properties of the homodyne optical states.

The compatibility of the purity parameters, obtained either by integrating the optical tomograms or extracted by saturating the uncertainty relation, that will be discussed in a forthcoming paper for different types of quantum states, can serve as a further test for evaluating the accuracy of the homodyne detection of the photon state.

We point out that the measured tomographic uncertainty function given in Fig. 3 contains important information. The value obtained for the function confirms the mixed state bound of the uncertainty relation. Moreover, it provides estimations of the purity parameter, the temperature and the mean photon number of the quantum thermal state.

Further study of other photon states like squeezed states and multi-mode states will give the possibility to check other quantum phenomena as higher momenta uncertainty relations.

Acknowledgements V.I. Man'ko thanks the University 'Federico II' and the Sezione INFN di Napoli for kind hospitality and the Russian Foundation for Basic Research for partial support under Projects No. 09-02-00142.

[1] P. van Lock, Fortschr. Phys. **50**, 1177 (2002);

[2] E. Schrödinger, Ber. Kgl. Akad. Wiss. Berlin, 296 (1930);

- [3] H. P. Robertson, *Phys. Rev.* **35**, 667 (1930);
- [4] W. Heisenberg, *Z. Phys.* **43**, 172 (1927);
- [5] V. V. Dodonov, V. I. Manko, *Proceedings of the P.N. Lebedev Physical Institute*, Vol. 183 (Nova Science, New York 1989);
- [6] V. V. Dodonov, *J. Opt. B: Quantum semiclass. Opt.* **4**, S98 (2002);
- [7] V. I. Man'ko, G. Marmo, A. Simoni, F. Ventriglia, *Adv. Sci. Lett.*, **2**, 517 (2009);
- [8] A. Ibert, V. I. Man'ko, G. Marmo, A. Simoni, and F. Ventriglia, *Physica Scripta*, **79**, 065013 (2009);
- [9] D. T. Smithey, M. Beck, M. G. Raymer, A. Faridani, *Phys. Rev. Lett.* **70**, 1244 (1993);
- [10] J. Mlynek, *Phys. Rev. Lett.* **77**, 2933 (1996);
- [11] A. I. Lvovsky, H. Hansen, T. Alchele, O. Benson, J. Mlynek, and S. Schiller, *Phys. Rev. Lett.* **87**, 050402 (2001);
- [12] V. D'Auria, S. Fornaro, A. Porzio, S. Solimeno, S. Olivares, and M. G. A. Paris, *Phys. Rev. Lett.* **102**, 020502 (2009);
- [13] T. Kiesel, W. Vogel, V. Parigi, A. Zavatta and M. Bellini, *Phys. Rev. A* **78**, 021804 (2008);
- [14] A. I. Lvovsky, and M. G. Raymer, *Rev. Mod. Phys.*, **81**, 299 (2009);
- [15] Paris, M., and J. Řeháček, Eds., *Quantum State Estimation*, Lecture Notes in Physics Vol. 649 Springer, Berlin (2004);
- [16] J. Kiukas, P. Lahti, J. Schultz, *Phys. Rev. A* **79**, 052119 (2009);
- [17] S. Mancini, V. I. Man'ko and P. Tombesi, *Phys. Lett. A* **213**, 1 (1996);
- [18] J. Bertrand and P. Bertrand, *Found. Phys.* **17**, 397 (1987);
- [19] K. Vogel and H. Risken, *Phys. Rev. A* **40**, 2847 (1989);
- [20] V. D'Auria, S. Fornaro, A. Porzio, E.A. Sete and S. Solimeno, *Appl. Phys. B* **91**, 309 (2008);
- [21] D. Buono, G. Nocerino, V. D'Auria, A. Porzio, S. Olivares, and M. G. A. Paris, *J. Opt. Soc. Am. B*, **27**:A110 (2010);
- [22] V. D'Auria, A. Chiummo, M. De Laurentis, A. Porzio, S. Solimeno, M. Paris, *Opt. Express* **13**, 948 (2005);
- [23] V. D'Auria, C. de Lisio, A. Porzio, S. Solimeno and M.G.A. Paris, *J. Phys. B: At. Mol. Opt. Phys.* **39**: 1187–1198 (2006);
- [24] J. Řeháček, S. Olivares, D. Mogilevtsev, Z. Hradil, M. G. A. Paris, S. Fornaro, V. D'Auria, A. Porzio, and S. Solimeno, *Phys. Rev. A* **79**, 032111 (2009);
- [25] G. M. D'Ariano, C. Macchiavello and M. G. A. Paris, *Phys. Rev. A* **50**, 4298 (1994);
- [26] A. Mandilara, E. Karpov, and N. J. Cerfl, *Phys. Rev. A* **79**, 062302 (2009).
- [27] The tomographic value is the one giving the lower error due the very high statistical reliability of such quantum state reconstruction method.